Clinical Science (2018) **132** 475–488
https://doi.org/10.1042/CS20171521

PORTLAND PRESS

Research Article

Short-term early exposure to thirdhand cigarette smoke increases lung cancer incidence in mice

Bo Hang[1,*], Yunshan Wang[1,2,*], Yurong Huang[1], Pin Wang[1,3], Sasha A. Langley[1], Lei Bi[1], Altaf H. Sarker[1], Suzaynn F. Schick[4], Christopher Havel[5], Peyton Jacob III[5], Neal Benowitz[6], Hugo Destaillats[7], Xiaochen Tang[7], Yankai Xia[8], Kuang-Yu Jen[9], Lara A. Gundel[7], Jian-Hua Mao[1,10] and Antoine M. Snijders[1,10]

[1]Biological Systems and Engineering Division, Lawrence Berkeley National Laboratory, Berkeley, CA 94720, U.S.A.; [2]International Biotechnology R&D Center, Shandong University School of Ocean, Weihai, Shandong 264209, China; [3]Department of Gastroenterology, Nanjing Drum Tower Hospital, Nanjing University Medical School, Nanjing, Jiangsu 210008, China; [4]Department of Medicine, Division of Occupational and Environmental Medicine, University of California, San Francisco, Box 0843, San Francisco, CA 94143, U.S.A.; [5]Division of Clinical Pharmacology and Experimental Therapeutics, Department of Medicine University of California, San Francisco, Box 0843, San Francisco, CA 94143, U.S.A.; [6]Division of Clinical Pharmacology and Experimental Therapeutics, Medical Services, Department of Medicine, and Bioengineering & Therapeutic Sciences, University of California, San Francisco, Box 0843, San Francisco, CA 94143, U.S.A.; [7]Indoor Environment Group, Energy Technologies Area, Lawrence Berkeley National Laboratory, Berkeley, CA 94720, U.S.A.; [8]State Key Laboratory of Reproductive Medicine, Institute of Toxicology, Nanjing Medical University, Nanjing 211166, China; [9]Department of Pathology and Laboratory Medicine, University of California Davis Medical Center, Sacramento, CA 95817, U.S.A.; [10]Berkeley Biomedical Data Science Center, Lawrence Berkeley National Laboratory, Berkeley, CA 94720, U.S.A.

Correspondence: Jian-Hua Mao (JHMao@lbl.gov) or Antoine M. Snijders (AMSnijders@lbl.gov)

Exposure to thirdhand smoke (THS) is a recently described health concern that arises in many indoor environments. However, the carcinogenic potential of THS, a critical consideration in risk assessment, remains untested. Here we investigated the effects of short-term early exposure to THS on lung carcinogenesis in A/J mice. Forty weeks after THS exposure from 4 to 7 weeks of age, the mice had increased incidence of lung adenocarcinoma, tumor size and, multiplicity, compared with controls. *In vitro* studies using cultured human lung cancer cells showed that THS exposure induced DNA double-strand breaks and increased cell proliferation and colony formation. RNA sequencing analysis revealed that THS exposure induced endoplasmic reticulum stress and activated p53 signaling. Activation of the p53 pathway was confirmed by an increase in its targets p21 and BAX. These data indicate that early exposure to THS is associated with increased lung cancer risk.

Introduction

Cigarette smoke, including both mainstream and secondhand smoke (SHS), is a rich source of mutagens and carcinogens such as *N*-nitrosamines, aromatic amines, aldehydes, polycyclic aromatic hydrocarbons (PAHs), and others [1-3]. Active smoking and SHS exposure both cause lung cancer [4-6]. SHS is produced by the combination of diluted sidestream smoke (emitted by a burning tobacco product) and exhaled mainstream smoke. It is very likely that the general mechanisms underlying lung cancer development by mainstream smoke and SHS are similar because the same carcinogens are found in both, albeit the carcinogen dose from SHS exposure is significantly lower than that from mainstream smoking [4].

Recently a new type of tobacco exposure, referred to as 'thirdhand smoke' (THS), has been identified. THS is defined as the pollutants that remain on indoor surfaces and in dust long after tobacco has been smoked [7,8]. Some of the adsorbed constituents can be re-emitted into the gas-phase and/or react with other pollutants to form more hazardous compounds. THS-exposed dust can also be re-suspended into the air. Fieldwork in the U.S. and China confirms the widespread presence of THS in indoor environments [8,9]. THS exposure occurs through the involuntary inhalation, ingestion or dermal uptake of aged residues from SHS. However, the timescale for exposure to THS pollution is generally much longer than for SHS, and could stretch to days, months or even years (long-term, low-level exposure). Traditional cleaning methods cannot remove THS pollution effectively.

*These authors contributed equally to this work.

Received: 13 November 2017
Revised: 02 February 2018
Accepted: 09 February 2018

Accepted Manuscript Online: 12 February 2018
Version of Record published: 28 February 2018

Clinical Science (2018) **132** 475–488
https://doi.org/10.1042/CS20171521

Studies in recent years have also shown that THS contains many types of toxic constituents, including volatile (VOCs) and semi-volatile organic compounds (SVOCs) that slowly reemit into the air, thus increasing exposure risk for nonsmokers [7,8,10]. Some of the chemical constituents identified in THS are known carcinogens that are the same as those present in the mainstream smoke and SHS such as polycyclic aromatic hydrocarbons (PAHs) and TSNAs (tobacco specific nitrosamines). Through an analysis of unpublished results from Philip Morris, Schick and Glantz reported that SHS can become more toxic and concentrations of carcinogenic TSNAs can increase over time [11]. Sleiman *et al.* later showed that nicotine, a main constituent of tobacco smoke, reacts with ozone (O_3) to yield aldehydes and nanoparticles [12] and with nitrous acid (HONO) to form several TSNAs, including 1-(*N*-methyl-*N*-nitrosamino)-1-(3-pyridinyl)-4-butanal (NNA), *N*-nitroso nornicotine (NNN) and 4-(methylnitrosamino)-1-(3-pyridinyl)-1-butanone (NNK) [13]. The extent of surface loading of TSNAs was estimated to be large enough to warrant investigation of health effects of exposure to THS [13]. Recent data from Schick and Glantz show that the majority of nicotine, cotinine, semi-volatile organics, PAHs and TSNAs that are released during smoking in buildings adsorb or deposit on room surfaces. As long as there are sources of the indoor pollutant HONO, reaction with adsorbed nicotine forms more TSNAs. These findings suggest that exposure to toxic and carcinogenic compounds such as PAHs and TSNAs in THS may contribute to smoking-attributable morbidity and mortality [14] through dermal absorption and inhalation of contaminated dust.

Compelling evidence now shows how THS and its specific constituents such as TSNAs can cause significant cellular and tissue changes at realistic doses. Exposure to THS generated in laboratory systems can cause significant DNA damage in human cell lines [15], higher levels of oxidative base lesions in skin wounds of mice [16], damage to multiple organs and alterations in body weight, immunity, and behavior in mice [17,18]. Exposure to THS at very low concentrations also caused distinct metabolic changes in mouse male reproductive cell lines [19]. It is well understood that the environmental pollutants that play key roles in the etiology of human cancer include chemical carcinogens, such as those in cigarette smoke. However, at present there is no direct evidence on the role of THS exposure in the development of tumors in animals and/or humans.

Compared with adults, small children face greater health risks from THS exposure because they typically spend more time indoors and have age-specific behaviors that bring them in close contact with surfaces and dust (i.e., crawling, mouthing, and/or ingesting non-food items). Moreover, children are more sensitive than adults to pollutants for several reasons: increased respiration rate/body size, larger exposed surface area/volume ratio, thinner skin, immaturity of immunologic systems, and low metabolic capacity. Thus even low doses of THS constituents may represent long-term health hazards to them [7,8]. Matt et al. reported that the homes of parents who only smoked outdoors still had higher levels of nicotine than the homes of nonsmokers, and more importantly, the children of parents who never smoked inside their home had higher urinary cotinine levels than the children of nonsmokers [20]. Even in places where smoking bans are strictly enforced, such as neonatal intensive care units in hospitals, THS can be found by measuring ratios of concentrations of (4-(methylnitrosamino)-1-(3-pyridyl)-1-butanol) (NNAL) to cotinine in infants' urine [21]. By analyzing nicotine and nitrosamines/TSNAs in house dust samples, Ramirez et al. found that exposure to nitrosamines increases cancer risk in non-smokers [22]. We recently investigated the effects of neonatal and adult THS exposure on bodyweight and blood cell populations in C57BL/6J mice and found that THS-treated mice had significantly lower bodyweight than their respective control mice in the neonatal period [18]. Although these results suggest that THS is a potential health threat to infants and young children, virtually nothing is known about the long-term effects of early-life THS exposure on cancer risk later in life.

The objective of this study was to test the hypothesis that short-term early exposure to THS increases the incidence of lung adenocarcinoma in A/J mice later in life, and to delineate the molecular and cellular mechanisms that underlie THS-induced tumorigenicity.

Materials and methods

THS sample preparation and characterization

For testing THS carcinogenicity in animals and other cellular experiments using cell lines, a controlled laboratory system was used to generate THS samples on cotton terry cloth, an approach developed in our previous work [15]. The cloth substrates were used as surrogates for indoor surfaces, onto which fresh SHS gases could adsorb and SHS particles deposit. Briefly, Clean 100% cotton terrycloth samples were repeatedly exposed to SHS in a 6-m^3 stainless steel chamber for a total of 234 h over 1019 days. During smoking, a total of 2795 mg of total particulate material was introduced into the steel chamber. This is equivalent to the smoke from 200 to 350 cigarettes over 2 years and 9 months, or approximately 1/5–1/3 of a cigarette per day. If all THS mass deposited on the surfaces of the exposure

chamber, the maximum loading of THS on each gram of cotton cloth would be 238 μg. The THS cloth was removed from the smoke, vacuum-packed in Mylar film and stored at −20°C until use.

Preparation of THS extracts

For chemical analysis and cell culture, THS-laden and unexposed (control) cotton cloth samples were weighed, cut into small pieces and immersed in Dulbecco's Modified Eagle's Medium (DMEM) using 0.85 g cloth material per 10 ml of medium, then vortexed and centrifuged as previously described [15]. One ml of media with THS and another without (control) were taken out and stored at 4°C until use. A collection of 12 targeted THS compounds in the DMEM samples was analyzed following the procedures described in the previous study [15], using liquid chromatography–tandem mass spectrometry (LC–MS/MS) as described in Whitehead *et al.* [23]. For PAHs analysis, 2.5 x 5 cm specimens of the THS-impregnated and unexposed (control) cloth samples were extracted with dichloromethane (DCM) by sonication for 30 min. Specimens were pre-spiked with a known amount of deuterated PAH standards (naphthalene-D8, phenanthrene-D10, anthracene-D10, pyrene-D10, and benzo[e]pyrene-D12) to assess recovery efficiency. Extraction was carried out using two identical 15 ml DCM aliquots sequentially. These extracts were analyzed separately to evaluate extraction efficiency. Duplicate DCM extracts were analyzed by gas chromatography coupled with mass spectrometry (GC/MS, Varian 4000, CA), using mixtures of PAH as quantification standards.

Mice exposed to THS and tumorigenesis

All animal experiments were performed at the Lawrence Berkeley National Laboratory and the study was carried out in strict accordance with the Guide for the Care and Use of Laboratory Animals of the National Institutes of Health. The animal use protocol was approved by the Animal Welfare and Research Committee of the Lawrence Berkeley National Laboratory.

A/J mice were divided into experimental (24 mice) and control (19 mice) groups, with 4 mice per cage. The experimental group was exposed to THS from 4 to 7 weeks of age; the control group was never exposed to THS. All mice were fed a standard chow diet (with caloric content of: 58% carbohydrate, 28.5% protein, and 13.5% fat). THS-exposed cloth was added to the standard bedding in the cages, and the cloth swatches were replaced once a week during the standard cage change. The cloth was the sole source of THS exposure. And only after the exposure period was the bedding switched back to the standard. There was 0.85 g (5×5 cm^2 swatch) of THS-exposed cloth per cage, with a nicotine loading of 30.6 μg/g and an upper limit for THS deposition of 238 μg/g (Table 1). Assuming that the uptake of nicotine through ingestion, inhalation, and dermal routes was quantitative, the predicted dose was 77 μg/day kg of bodyweight. This value is comparable to the ingestion exposure of a toddler estimated by Bahl et al. [24]. Control animals were housed separately on standard bedding. Lung tumor incidence, size, and multiplicity were determined 40 weeks after THS exposure. All tumors were embedded for histopathological evaluation.

Cell culture

Human lung cancer cell lines NCI-H460, NCI-H510, and NCI-A549 were purchased from ATCC (Manassas, VA). NCI-H460 cells were maintained in RPMI-1640 medium with 10% fetal bovine serum (FBS). The NCI-H510 and NCI-A549 cells were maintained in F-12K medium with 10% FBS. All cells were grown at 37°C with 5% CO_2 in air. THS-laden DMEM was prepared as above and diluted in complete culture medium. The culture medium was replaced every three days with fresh THS or control supplemented culture media.

RNA isolation and sequencing

Total RNA was isolated utilizing the RNeasy mini kit (Qiagen) and DNA was removed using RNase-free DNase (Qiagen). RNA quality was assessed using a BioAnalyzer. RNA sequencing was performed at the UCLA Technology Center for Genomics & Bioinformatics (TCGB). RNA-sequencing reads were mapped to the human genome (GRCh38 reference, including alt contigs, decoy and EBV sequences; downloaded from the 1000 Genomes Project) using STAR v2.5.2b [25], default parameters. For each replicate, per-gene counts of uniquely mapped reads were computed using HTSeq 0.6.1p2 [26] and Gencode v26 [27] primary assembly annotations. Differential expression analysis was performed and normalized gene counts were generated using DESeq2 v1.16.1 [28]. Heatmaps were created using the gplots v3.0.1 R package.

Clinical Science (2018) **132** 475–488
https://doi.org/10.1042/CS20171521

Table 1 Concentrations of THS constituents in the cotton cloth used as mouse bedding material

Compound	LOQ[1]	THS sample	Control sample
Nitrogenated species (ng/g)			
Nicotine	12	30600	14.9
Cotinine	12	486	BLQ[2]
3-EP[3]	12	131	BLQ
N-FNNIC[4]	12	998	BLQ
NNK[5]	5.9	BLQ	BLQ
NNN[6]	1.2	3.54	BLQ
NNA[7]	1.2	11.9	BLQ
Myosmine	24	2440	BLQ
NAT	1.2	BLQ	BLQ
2,3-Bipyridine	2.4	439	BLQ
NAB[8]	1.2	BLQ	BLQ
Nicotelline	5.9	12.6	BLQ
Polycyclic aromatic hydrocarbons, PAHs (ng/g)			
Naphthalene	2	27	BLQ
1-Methyl naphthalene	3	10	BLQ
2-Methyl naphthalene	2	27	BLQ
Acenaphthylene	1	2	BLQ
Acenaphthene	1	4	BLQ
Fluorene	1	3	BLQ
Phenanthrene	2	18	BLQ
Anthracene	2	3	BLQ
Fluoranthene	1	10	BLQ
Pyrene	1	24	BLQ
Chrysene	1	9	BLQ
Benzo[a]anthracene	1	8	BLQ
THS mass (μg/g)			
Upper limit of THS deposition[9]	39	238	BLQ

[1]LOQ = limit of quantitation.
[2]BLQ = below limit of quantitation.
[3]3-EP: 3-ethenyl-pyridine.
[4]N-FNNIC: *N*-formylnornicotine.
[5]NNK: 4-(methylnitrosamino)-1-(3-pyridyl)-1-butanone.
[6]NNN: *N*-nitroso nornicotine.
[7]NNA: 4-(methylnitrosamino)-1-(3-pyridyl)-1-butanal.
[8]NAB: *N*-nitroso anabasine
[9]THS mass: upper limit of deposition of THS, μg/g of cotton.

Quantitative RT-PCR (qRT-PCR)

Total RNA samples were extracted from lung cancer tissues (Invitrogen). cDNA was synthesized from 1 μg of total RNA with One Step RT-PCR Kit (TaKaRa). qRT-PCR was performed with the SYBR Green (TaKaRa) detection method on an ABI-7500 RT-PCR system (Applied Biosystems) using the following primers: CEBPB (Forward primer: AGCGACGAGTACAAGATCCG; Reverse primer: CATGTGCGGTTGGTTTGGAC), SLC7A11 (Forward primer: TGCCCAGATATGCATCGTCC; Reverse primer: TCAACCCGCGGTACTCTTTC), NUPR1 (Forward primer: TCATGCCTATGCCCACTTCA; Reverse primer: CCGCAGTCCCGTCTCTATTG), GDF15 (Forward primer: GGTGTCGCTCCAGACCTATG; Reverse primer: GGAACCTTGAGCCCATTCCA).

Western blotting

Cells were homogenized in RIPA lysis buffer supplemented with protease inhibitors. Protein concentration was measured by the Bradford protein assay (Bio-Rad). The samples were prepared for loading by adding 4X sample buffer and heating the sample at 95°C for 5 min. Total proteins were separated by SDS-PAGE, transferred to PVDF membrane and analyzed by immunoblotting as previously described [29]. Membranes were probed with the following antibodies: anti-p53, anti-p-p53, anti-p21, anti-Bax (Abcam), and anti-β-actin (Cell signaling). Anti-rabbit-HRP and anti-mouse-HRP secondary antibodies (Sigma) were used.

γ-H2AX immunofluorescence

Cells were plated on glass coverslips in 24-well plates for 12 h and then treated with varying concentrations of THS extract (1:20, 1:80, 1:160, 1:320, and control) for 24 h. The cells were washed with cold PBS and fixed with 2% PFA for 30 min at room temperature. The cells were permeabilized for 30 min in 0.2% Triton X-100. Then cells were washed three times in staining buffer (1% BSA, 22.52 mg/ml glycine, 0.1% Tween 20 in PBS) incubated for 30 min in staining buffer at room temperature, incubated with anti-γH2AX (Abcam) overnight at 4°C, washed three times in staining buffer, incubated with second antibody for 1 h at room temperature, and washed three times with PBS. Next, the cells were stained with DAPI for 10 min, washed with PBS and mounted in Vectashield (Vectorlabs). The samples were examined using a Zeiss Axio Observer Z.1 inverted microscope combined with LSM 780 confocal module with a 40× oil objective.

Cell proliferation and colony formation assays

For cell proliferation, cells were seeded in 96-well plates in triplicate at densities of 1×10^3 per well. Cell proliferation was monitored using MTT (Sigma) (5 mg/ml) for 4 h. Light absorbance of the solution was measured at 570 nm on a microplate reader (Bio-Rad). For colony formation, cells were seeded in triplicate at 500 cells/6-cm dish in complete medium. After 3 weeks of growth, the cells were fixed and stained with 0.1% crystal violet (Sigma), and visible colonies were counted according to cell numbers in each colony using a microscope (Zeiss, Axio Vert.A1).

Soft agar assay

For anchorage-independent growth in soft agar, the bottom layer was obtained by covering a six-well plate with 2 ml of 0.5% agar in medium. On the next day, 1×10^3 cells were plated on this bottom layer in 2 ml of 0.34% agar. Colonies were counted after 3 weeks using a microscope.

Migration and invasion assay

Cells were plated in a trans-well migration chamber with 8 μm pores (BD Biosciences) in serum-free medium and allowed to migrate towards medium containing 10% FBS for 24 h. Cells that had migrated through the membrane were fixed, stained, and counted. For invasion assays the migration chambers were pretreated with 50 μl Matrigel (BD Biosciences) at 1 mg/ml.

Statistical analysis

Data were described as the mean ± S.D. Comparisons between different groups were undertaken using the Student's two-tailed *t* test. The limit of statistical significance was $P<0.05$. Statistical analysis was done with SPSS/Win11.0 software (SPSS, Inc., Chicago, Illinois, USA).

Data availability

RNA-Seq data have been deposited at NCBI SRA under accession code SUB2987635.

Results

THS exposure increases lung cancer incidence in mice

To test the tumorigenic potential of exposure to THS during development, we exposed A/J mice to THS as shown in Figure 1a and described in the Materials and Methods. After 3 weeks of THS treatment, mice were monitored for 40 weeks until lung tumor evaluation at 47 weeks of age. We found a significant increase in the proportion of THS-treated mice with lung tumors, compared with control mice (Figure 1b; $P=0.026$). Moreover, the tumors from THS-treated mice were larger than those from control mice; some of them reached 2 mm (Figure 1c; Supplementary Table S1). In addition, 3 of 12 THS-treated tumor-bearing mice developed multiple lung tumors (more than 3) while none of control mice did so (Supplementary Table S1). Histological evaluation classified the lung tumors as adenocarcinoma (Figure 1c and Supplementary Figure S1).

THS sample generation, extraction, and chemical characterization

To identify potential carcinogenic compounds in the THS-exposed cotton terry cloth we used a water-based extraction, i.e., DMEM, to determine the concentrations of chemical compounds in the samples that were used as bedding material in the mouse cages. Table 1 summarizes the compounds detected and quantified in the THS-treated DMEM and DMEM-only samples using the LC–MS/MS procedure. Nicotine was the main component detected in

Clinical Science (2018) **132** 475–488
https://doi.org/10.1042/CS20171521

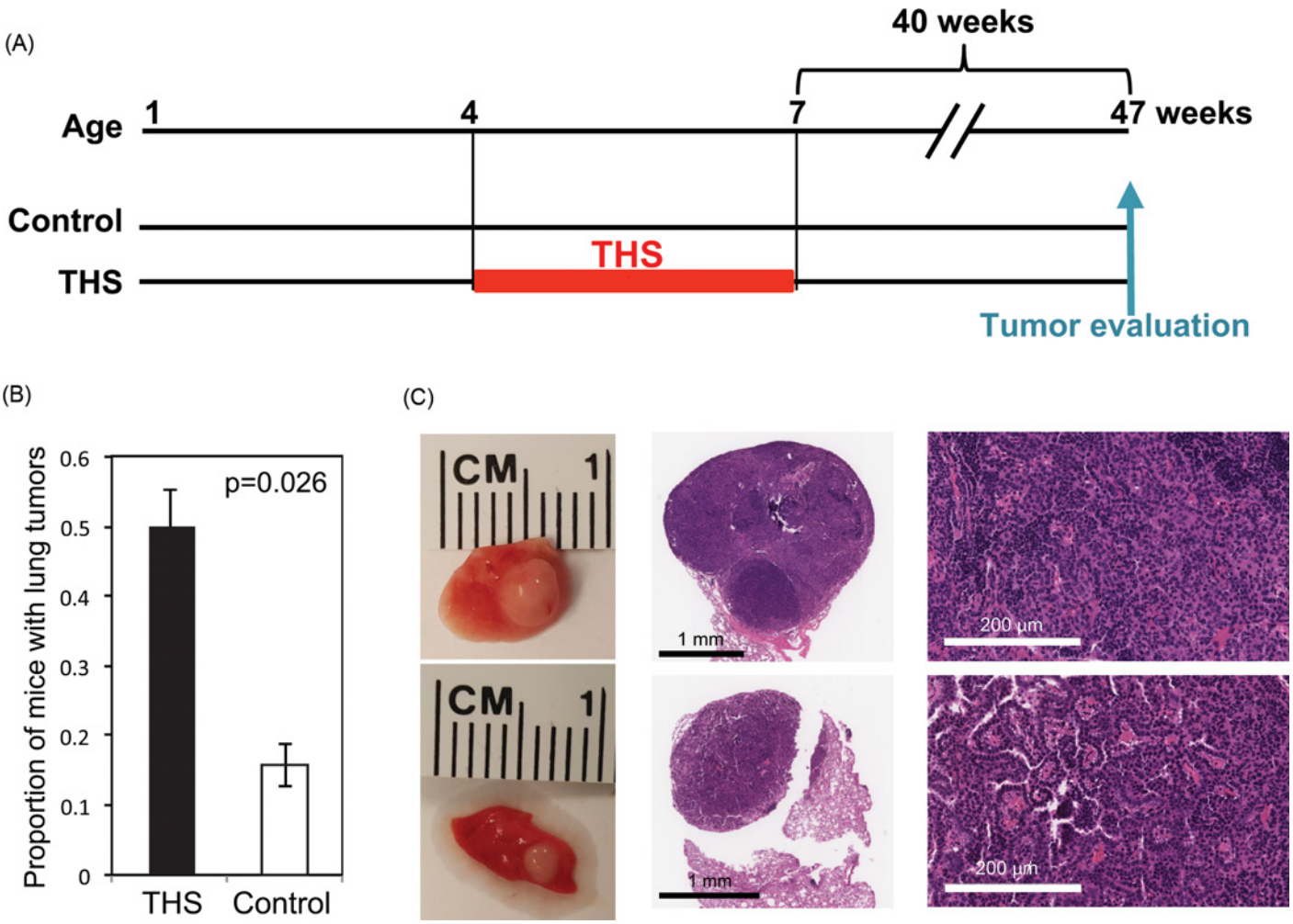

Figure 1. THS exposure increases lung cancer incidence in A/J mice

(**a**) Overview of experimental design. Mice were exposed from 4 to 7 weeks of age and lung tumor incidence was assessed 40 weeks after the end of exposure. (**b**) Proportion of mice with lung tumors in THS (black) and control (white) groups. The *P*-value was obtained using Chi-square test. (**c**) Representative images of lung tumors from THS exposed mice and their corresponding H&E stains.

the THS-treated samples. Other water-soluble nitrogenated compounds detected with varying levels include cotinine, 3-EP, two tobacco-specific nitrosamines (NNA and NNN), myosmine, 2,3-bipyridine, and nicotelline. All the compounds tested were below detection levels (BLQ) in the DMEM-only samples (control) except for trace amounts of nicotine (Table 1). Considerable variability can be expected for chemically reactive analytes such as TSNAs, 3-EP, myosmine and N-formylnornicotine. Factors affecting variability are: THS loading on the material, amount of liquid used in the extraction, formation of TSNAs during aging (*e.g.*, in the presence of HONO from smoking). Relative ratios among these analytes are comparable to those reported from other materials exposed in the same chamber [24]. Twelve PAHs were identified and quantified in the DCM extracts of THS-laden material, with a total PAH loading of approximately 130 ng per gram of cloth. In most cases, individual PAH concentrations were close to the limit of detection, suggesting that other PAHs may have been present at slightly lower levels and could not be analyzed by this method. Schick *et al.* [14] identified a total of 16 PAHs in the gas phase and particulate matter after smoking in the same chamber, which included the twelve analytes detected in the cloth THS sample. No PAHs were found in unexposed (control) cloth specimens.

THS exposure induces ER stress and activates p53 signaling

To begin to elucidate the molecular mechanisms associated with increased lung cancer incidence in THS-exposed mice, we exposed human H510 and H460 lung cancer cells to DMEM extracts of the THS-cloth ($n = 3$) or DMEM

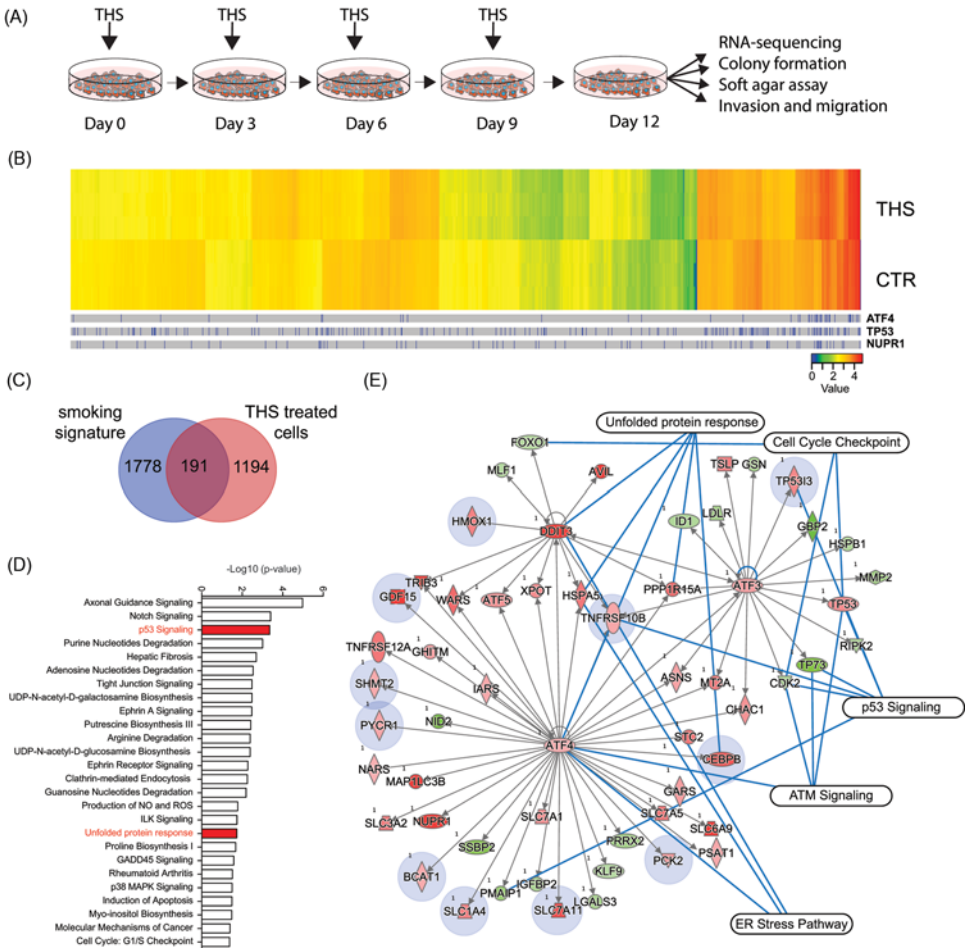

Figure 2. THS exposure alters expression of genes involved in ER stress and p53 signaling pathways

(**a**) Overview of *in vitro* experiments using human lung cancer cell lines (H460 and H510) treated with THS (1:80). The culture medium was replaced every three days with fresh THS or control supplemented culture media. (**b**) Heatmap of differentially expressed genes in H510 cells collected at day 12 (see Figure 2a). Genes regulated by ATF4, TP53, and NUPR1 are indicated in blue bars underneath the heatmap. (**c**) Overlap of genes differentially expressed in H510 cells and a human smoking signature published previously [30]. (**d**) Canonical pathways significantly enriched in response to THS exposure in H510 cells. (**e**) Gene interaction network in response to THS exposure enriched for p53 and ER stress signaling. Genes up-regulated after THS exposure are highlighted in red; down-regulated genes are highlighted in green. Genes that are also deregulated in the published human smoking signature are further highlighted in purple.

alone ($n = 3$) for 12 consecutive days (Figure 2a). RNA-seq analysis of RNAs from THS-treated H510 cells revealed that THS exposure modulated 1502 transcripts (682 up-regulated and 820 down-regulated compared with the control; adj. $P<0.05$ and fold-change>1.5; Figure 2b; Supplementary Table S2), which corresponds to 1385 genes. THS induced change in gene expression was validated for some genes using qRT-PCR (Supplementary Figure S2). Since some compounds found in THS are also present in mainstream smoke, not surprisingly, we found a significant overlap with a published non-tumor human lung tissue smoking signature (Figure 2c; $P<0.01$) [30], suggesting that at least part of the *in vitro* transcriptional response to THS is similar to transcriptional changes in active smokers. We next mapped the 1385 differentially expressed genes to biological functions, pathways and upstream transcriptional regulators using Ingenuity Pathway Analysis for the computations. We observed significant enrichment of p53 signaling and integrated stress response pathways and genes regulated by TP53, ATF3, ATF4 NUPR1, and DDIT3 in THS-exposed cells (Figure 2d,e; Supplementary Table S3). ATF4 and DDIT3 up-regulation indicate activation of the integrated stress response to accumulation of unfolded proteins in the endoplasmic reticulum, amino acid starvation, or oxidants.

Clinical Science (2018) **132** 475–488
https://doi.org/10.1042/CS20171521

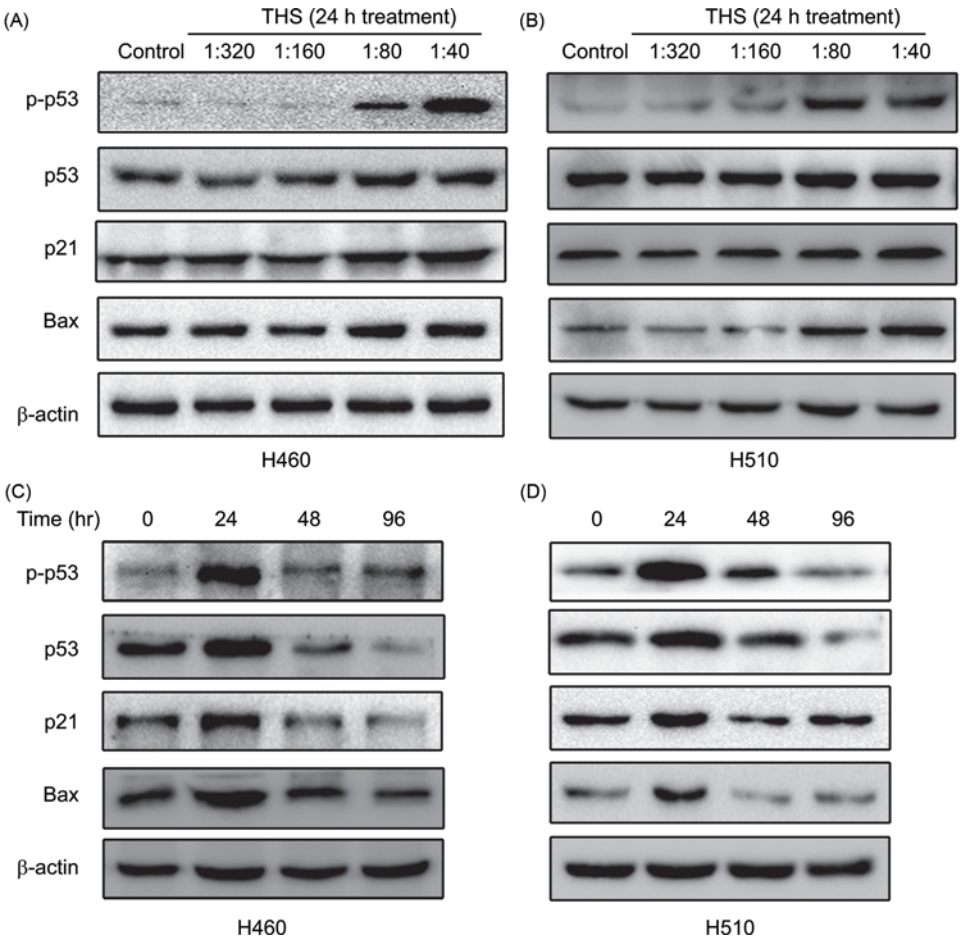

Figure 3. Dose- and time-dependent effects of THS on p53 signaling pathway

(**a–b**) Dose-dependent activation of p53 signaling pathway in H460 cells (**a**) and H510 cells (**b**) 24 hours after THS exposure. (**c–d**) Time-dependent effect of THS (1:40 dilution) on p53 signaling pathway in H460 cells (**c**) and H510 cells (**d**) at 24, 48, and 96 h after exposure.

Activation of p53 pathway by THS exposure

To test whether p53 is activated by THS exposure we examined p53 protein stability and phosphorylation in human H460 and H510 lung cancer cell lines. We treated cells for 24 h at THS extract dilutions ranging from 1:40 to 1:320. We found that the total protein level of p53 was not affected by THS treatment. However, an increase in phosphorylation at Ser15 was observed in a dose dependent manner at 1:40 and 1:80 THS dilutions (Figure 3a,b). Protein levels of the p53 transcriptional targets p21 and BAX were also increased at 1:40 and 1:80 THS dilutions. To determine the persistence of p53 activation we measured phosphorylated p53, p21, and BAX in H460 and H510 cells treated with THS at a 1:40 dilution for 24, 48 and 96 h time points. Phosphorylated p53, p21, and BAX increased sharply at 24 h, after which levels returned to baseline at 96 h (Figure 3c,d). Finally, similar results were observed in the human lung adenocarcinoma cell line A549 (Supplementary Figure S3a) and lung tissues from mice exposed to THS (Supplementary Figure S4).

THS exposure induces DNA double-strand breaks

Previous studies using the comet assay showed that exposure of human liver HepG2 cells to THS for 24 h resulted in significant increases in DNA strand breaks [15]. To test whether or not THS induces DNA double-strand breaks (DSBs) in human lung cells, we treated H460 and H510 cancer cells with THS at dilutions ranging from 1:40 to 1:320 for 24 h and measured γ-H2AX foci (Figure 4a). Histone H2AX is specifically phosphorylated at the sites of DSBs, and antibodies against phospho-H2AX (γ-H2AX) have been developed to pinpoint the sites of DSBs [31]. We observed a dose-dependent increase in the number of cells with more than 5 foci compared with controls (Figure 4b). The treated

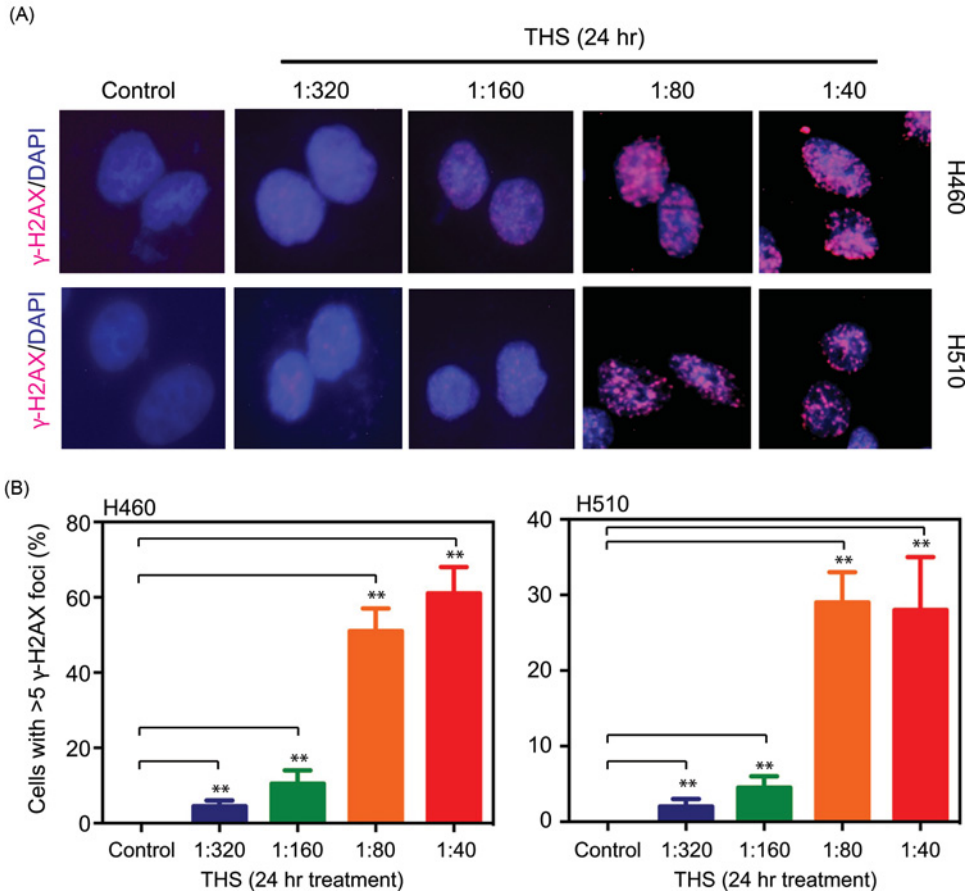

Figure 4. Dose-dependent increase in DNA double-strand breaks induced by THS

(**a**) Representative images of γ−H2AX foci staining 24 h after THS exposure across different doses. (**b**) Quantitation of γ-H2AX foci staining 24 h after THS exposure. Number of cells with more than five foci were counted. Significance was obtained using Chi-square test in comparison to control treated cells (** *P*-value<0.01).

cells had significantly higher levels of DSBs ($P<0.01$) compared with those of controls, even at the lowest dilution tested (1:320). This observation was also demonstrated in A549 cells (Supplementary Figure S3b).

THS exposure does not influence migration and invasion

We next examined whether 12-day continuous THS exposure increases tumorigenic properties of cells *in vitro* (Figure 2a). We first assessed the effects of THS exposure on the migration capability of THS-treated H460 and H510 cells related to tumor metastasis. We found that the migration of both cell lines did not increase significantly compared with control cells (Supplementary Figure S5a,b). In addition, cell invasion was not significantly enhanced by THS treatment either (Supplementary Figure S5c,d).

THS exposure increases growth and tumorigenic potential in vitro

We then assessed the effects of THS on cell proliferation and colony formation as described in the Methods section. THS-treated H460 (Figure 5a), H510 cells (Figure 5b) and A549 (Supplementary Figure S3c) exhibited increased cell proliferation compared with their control cells. Furthermore, THS-treated H460 and H510 cells exhibited significant increases in the number of colonies with >200 cells and total number of colonies compared with controls (Figure 5c,d).

THS exposure increases colony formation in soft agar

To measure anchorage-independent growth, a property of malignant cells, we assessed the effects of THS exposure on colony forming ability in soft agar in H460 and H510 cells. Cells were exposed for twelve consecutive days to THS

Clinical Science (2018) **132** 475–488
https://doi.org/10.1042/CS20171521

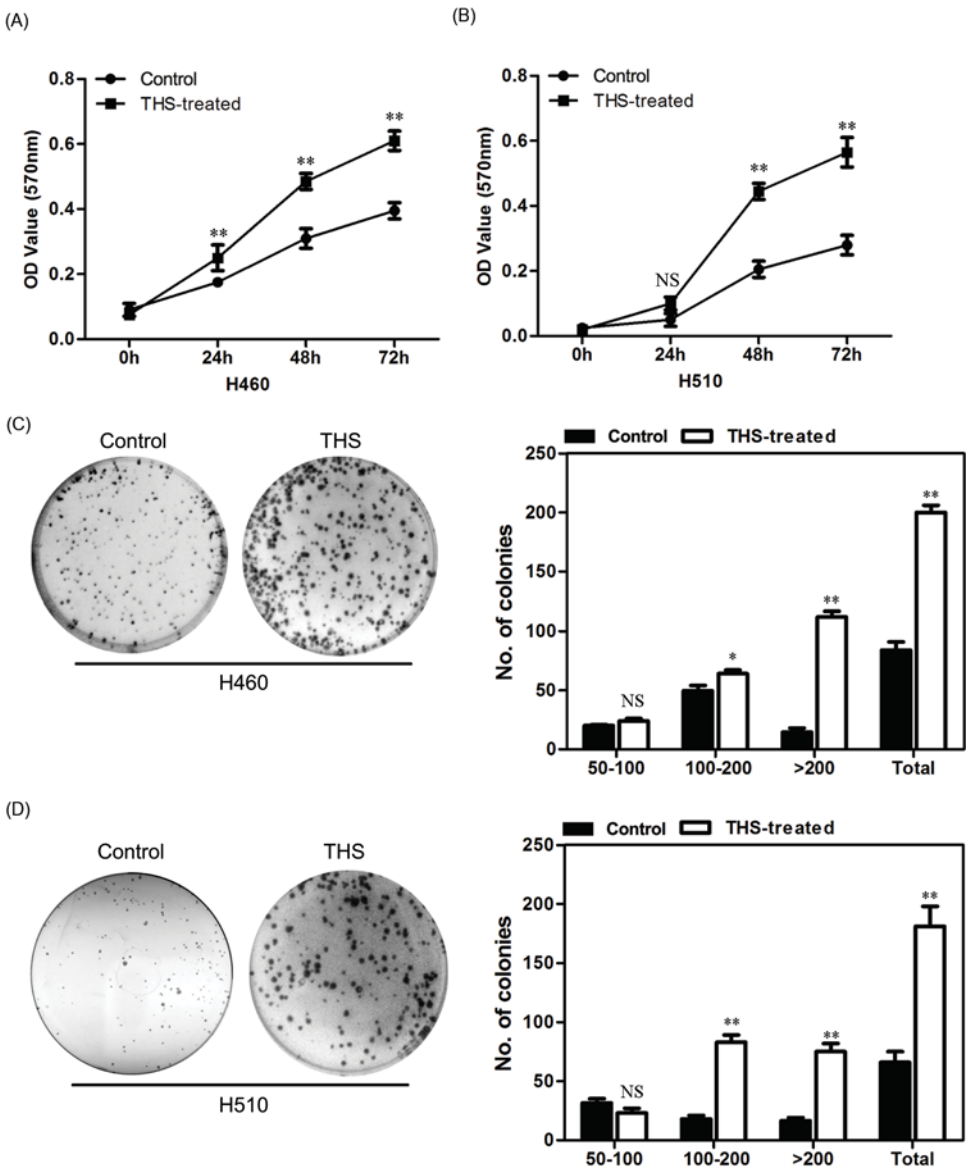

Figure 5. THS increases cell proliferation

(**a–b**) THS exposure (1:80) increases cell proliferation assessed by MTT assay in H460 cells (**a**) and H510 cells (**b**). Significance was obtained using t-test at each timepoint in comparison to control treated cells (* *P*-value<0.05; ** *P*-value<0.01). (**c–d**) THS exposure (1:80) increases clonogenic potential of H460 cells (**c**) and H510 cells (**d**). Representative cell culture plates of control and THS treated cells are shown on the left. Quantitation of the total number and relative size of individual colonies is shown on the right. Significance was obtained using Chi-square test in comparison to control treated cells (* *P*-value<0.05; ** *P*-value<0.01; NS: not significant)

in monolayer cultures after which cells were re-plated in soft agar (Figure 2a). We observed significant increases in the diameter and number of colonies in THS treated cell compared with control H460 and H510 cells (Figure 6a,b).

Discussion

In this work, we showed for the first time that THS exposure during early life (the juvenile period) significantly increases lung cancer incidence in A/J mice. Although current evidence, including animal studies, suggests that THS may be a potential health threat to infants and young children who are in smokers' homes, virtually nothing is known

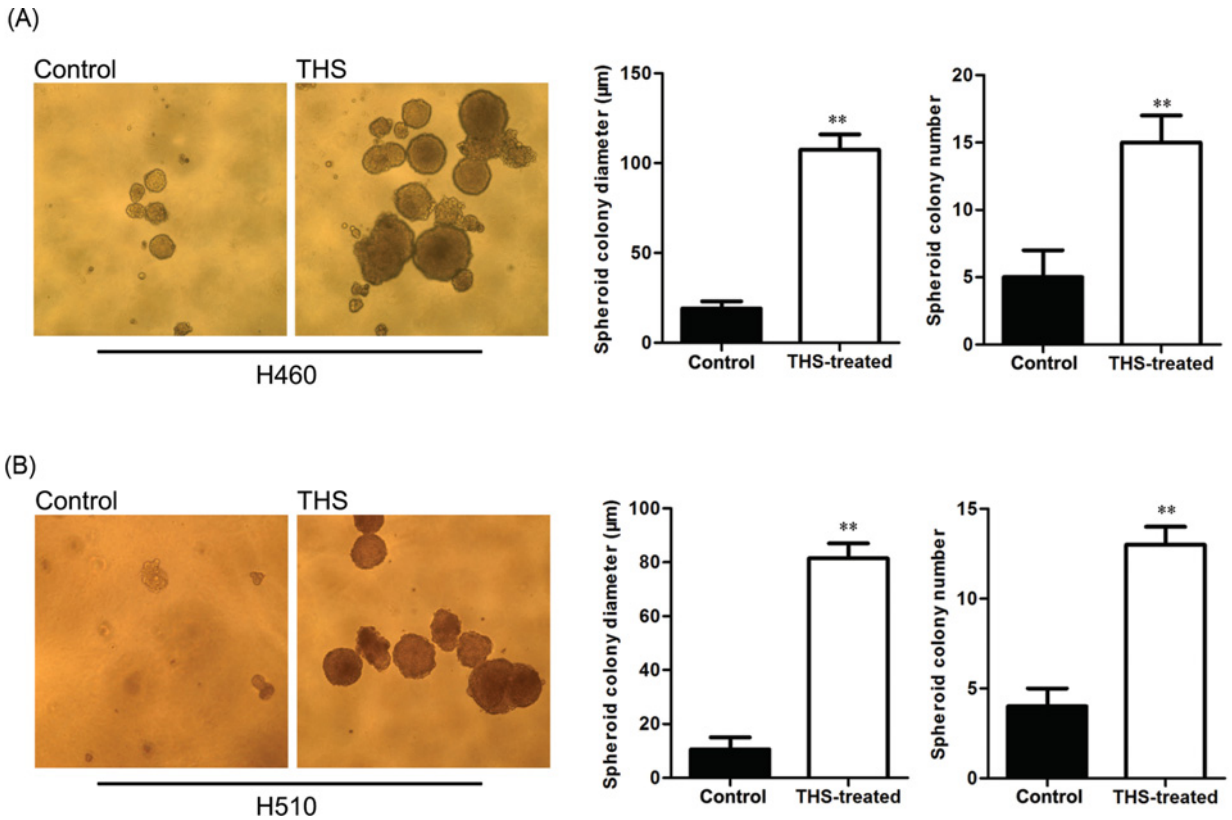

Figure 6. THS increases anchorage independent growth

THS exposure (1:80) increases anchorage independent growth in soft agar of H460 cells (**a**) and H510 cells (**b**). Representative images of control and THS treated cells are shown on the left. Quantitation of the size and total number of individual colonies is shown on the right. Significance was obtained using *t* test in comparison to control treated cells (** *P*-value<0.01).

about the long-term effects of early THS exposure on tumor development in later life. Some of the chemical constituents identified from THS are known carcinogens that are the same as those present in the mainstream smoke and SHS, such as PAHs and TSNAs, albeit at different concentrations. Interestingly, TSNAs can also be generated *de novo* in THS, as described before [13]. As for lung cancer induction, these two classes of chemical compounds have been shown to be potent carcinogens, among the multiple carcinogens convincingly identified from cigarette smoke to cause lung tumors in laboratory animals or humans [32]. Therefore, they are likely to play major roles in lung carcinogenesis by THS.

Diverse confounding factors in humans, such as genetic and environmental conditions, may limit our ability to draw definitive conclusions about the biological and health impacts of THS. In addition, currently it is very difficult to separate the effects of THS from SHS in human populations because most people who are affected by 'passive smoking' receive a mixed exposure to both SHS and THS. Mouse models offer many advantages for assessing health risks after THS exposure, because they allow control of both the genetic and environmental components of risk. The A/J mice strain is susceptible to spontaneous lung cancer development and has been a useful test system in the field of tobacco carcinogenesis, particularly in investigating lung cancer induced by specific carcinogens such as mainstream cigarette smoke and SHS [33-36].

The conditions used in our mouse exposure to THS were intended to mimic human exposures. Analysis of the THS samples used in our animal studies showed the presence of nicotine and carcinogens including TSNAs and PAHs (Table 1). Assuming that uptake of nicotine through ingestion, inhalation, and dermal routes was quantitative, the predicted dose was 77 μg/kg day of bodyweight. This value is comparable to the ingestion exposure of a toddler estimated by Bahl *et al.* [24]. Interestingly, all the concentrations including those of nicotine, cotinine, 2,3'-BP, TSNAs (NNA and NNN), nicotelline, myosmine, and N-formylnornicotine (Table 1) were several-fold lower than those reported by Bahl *et al*. for cell-culture based assays when the same extraction method was used [24], indicating that the exposure levels in our experiments were reasonable. It should be noted that the aqueous and organic extracts

Clinical Science (2018) **132** 475–488
https://doi.org/10.1042/CS20171521

that we analyzed may underestimate the actual exposure of the mice. Their ingestion and dermal exposure may have included TSNAs and PAHs that are not extractable in DMEM or DCM.

It is well known that tobacco carcinogens, such as those found in THS [8], generate a broad spectrum of DNA lesions ranging from sugar damage, oxidized bases and bulky base adducts to more deleterious lesions such as DNA strand breaks. Research has shown that formation of DNA adducts plays a central role in smoking-induced mutagenesis and carcinogenesis [37]. If DNA adducts are not repaired, they can cause miscoding during DNA replication, thus leading to mutations [37]. Our previous studies on DNA strand breaks and oxidative base damage [15,16] made important contributions to the initial understanding of the genotoxic effects of THS, and they raised concerns about the carcinogenic potential of exposure to THS. We also observed that NNA, which is highly selective for THS in environments with combustion sources, reacts with dG *in vitro* to form a bulky cyclic adduct [38].

Studying THS-induced DNA damage may provide mechanistic insight into how THS may cause neoplastic transformation. There are many studies that addressed the relationships between tobacco carcinogen exposure, DNA damage, mutagenic potential, and increased cancer risk related to smoking [37]. For example, PAH-DNA adducts are preferentially formed in the same mutational hotspots of *p53* as in the lung cancers of smokers [39]. This tumor suppressor gene is mutated in ∼40% of lung cancer cases [39]. Tobacco smoke also produces reactive oxygen species (ROS) and induces oxidative stress. The lesions that arise directly from ROS attack on a base, such as 8-oxoguanine (8-oxoG), could also play a role in tobacco carcinogenesis. We previously reported high levels of 8-oxoG and other oxidized lesions in mouse skin wounds exposed to THS [16]. Moreover, we demonstrated that THS exposure induces DNA strand breaks including DSBs. Mispair or lack of repair of a DSB can result in mutations or generate dicentric or acentric chromosomal fragments [40]. DSBs can also activate the p53 signaling pathway as evidenced by increased expression of the p53 targets p21 and BAX, as shown in this study. Therefore, one mechanism for THS-mediated carcinogenesis may be related to the formation of DSBs that can lead to genomic instability resulting in oncogenic transformation and increased cancer risk [41].

Clinical perspectives

- We investigated the effects of short-term early exposure to THS on lung carcinogenesis.
- This study demonstrates that exposure to THS during early life can increase lung cancer risk in A/J mice and that THS exposure induces DNA DSBs and enhances tumorigenic traits in human lung cancer cells.
- These data suggest that THS exposure is a potential risk factor for human lung cancer. Such information could be critical for preventing and controlling THS-induced biological and health harm, as well as for framing and enforcing new policies against indoor smoking in the U.S., China, and other countries.

Acknowledgements

The authors thank Marion Russell (LBNL) for support on PAH analysis.

Author contribution

J.H.M. B.H., and A.M.S conceived and designed the study and co-wrote the manuscript. J.H.M., B.H., Y.W., Y.H., P.W., L.B., A.H.S., Y.X., and A.M.S. performed the mouse experiments, acquired the data, and performed data analysis. S.A.L. performed RNA-sequencing data analysis and interpreted results. S.F.S., C.H., P.J., N.B., H.D., X.T., and L.A.G. generated and characterized THS material and co-wrote the manuscript. All authors read and approved the final manuscript.

Funding

This work was supported by the University of California Tobacco-Related Disease Research Program (TRDRP) [research project grants 24RT-0038 (to B.H. and J.H.M.) and 23PT-0013 (to H.D. and L.G.)]; the Lawrence Berkeley National Laboratory Directed Research and Development (LDRD) program funding (to J.H.M. and A.M.S.) under contract DE AC02-05CH11231; the National Institute on Drug Abuse [grant number P30 DA012393 (to P.J. III and N.B.)], and the National Center for Research Resources [grant

number S10 RR026437 (P.J. III and N.B.)], for laboratory resources at the University of California, San Francisco; the China Post-doctoral International Exchange Program 2015, National Science Foundation of China [grant number 81402193], the Postdoctoral innovation project of Shandong Province, and the Postdoctoral Science Foundation of China (to Y.S.W.).

Competing interests

Dr. Benowitz has been an expert witness in litigation against tobacco companies. The other authors declare no competing financial interests.

Abbreviations

DSB, double-strand break; LC–MS/MS, liquid chromatography–tandem mass spectrometry; NNA, 1-(*N*-methyl-*N*-nitrosamino)-1-(3-pyridinyl)-4-butanal; NNN, *N*-nitrosonornicotine; NNK, 4-(methylnitrosamino)-1-(3-pyridyl)-1-butanone; PAH, polycyclic aromatic hydrocarbon; SHS, secondhand smoke; THS, thirdhand smoke; TSNA, tobacco specific nitrosamine.

References

1 Hecht, S.S. (2003) Tobacco carcinogens, their biomarkers and tobacco-induced cancer. *Nat. Rev. Cancer* **3**, 733–744, https://doi.org/10.1038/nrc1190
2 Smith, C.J., Perfetti, T.A., Garg, R. and Hansch, C. (2003) IARC carcinogens reported in cigarette mainstream smoke and their calculated log P values. *Food Chem. Toxicol.* **41**, 807–817, https://doi.org/10.1016/S0278-6915(03)00021-8
3 California Environmental Protection Agency (2005) *Proposed Identification of Environmental Tobacco Smoke as a Toxic Air Contaminant*, California Environmental Protection Agency
4 International Agency for Research on Cancer (2003) *Tobacco Smoke and Involuntary Smoking*, International Agency for Research on Cancer, Lyon, France
5 Centers for Disease Control and Prevention (2004) *The Health Consequences of Smoking: A Report of the Surgeon General*, U.S. Department of Health and Human Services, Centers for Disease Control and Prevention, National Center for Chronic Disease Prevention and Health Promotion, Office on Smoking and Health, Atlanta, GA
6 Hecht, S.S. (2012) Lung carcinogenesis by tobacco smoke. *Int. J. Cancer* **131**, 2724–2732, https://doi.org/10.1002/ijc.27816
7 Matt, G.E., Quintana, P.J., Destaillats, H., Gundel, L.A., Sleiman, M., Singer, B.C. et al. (2011) Thirdhand tobacco smoke: emerging evidence and arguments for a multidisciplinary research agenda. *Environ. Health Perspect.* **119**, 1218–1226, https://doi.org/10.1289/ehp.1103500
8 Jacob, P., Benowitz, 3rd, N.L., Destaillats, H., Gundel, L., Hang, B., Martins-Green, M. et al. (2017) Thirdhand smoke: new evidence, challenges, and future directions. *Chem. Res. Toxicol.* **30**, 270–294, https://doi.org/10.1021/acs.chemrestox.6b00343
9 Zhang, S., Qiao, S., Chen, M., Xia, Y., Hang, B. and Cheng, S. (2015) A investigation of thirdhand smoke pollution in 3 types of places of Nanjing, 2014. *Zhonghua Yu Fang Yi Xue Za Zhi* **49**, 31–35
10 Sleiman, M., Logue, J.M., Luo, W., Pankow, J.F., Gundel, L.A. and Destaillats, H. (2014) Inhalable constituents of thirdhand tobacco smoke: chemical characterization and health impact considerations. *Environ. Sci. Technol.* **48**, 13093–13101, https://doi.org/10.1021/es5036333
11 Schick, S.F. and Glantz, S. (2007) Concentrations of the carcinogen 4-(methylnitrosamino)-1-(3-pyridyl)-1-butanone in sidestream cigarette smoke increase after release into indoor air: results from unpublished tobacco industry research. *Cancer Epidemiol. Biomarkers Prev.* **16**, 1547–1553, https://doi.org/10.1158/1055-9965.EPI-07-0210
12 Sleiman, M., Destaillats, H., Smith, J.D., Liu, C.-L., Ahmed, M., Wilson, K.R. et al. (2010) Secondary organic aerosol formation from ozone-initiated reactions with nicotine and secondhand tobacco smoke. *Atmos. Environ.* **44**, 4191–4198, https://doi.org/10.1016/j.atmosenv.2010.07.023
13 Sleiman, M., Gundel, L.A., Pankow, J.F., Jacob, 3rd, P., Singer, B.C. and Destaillats, H. (2010) Formation of carcinogens indoors by surface-mediated reactions of nicotine with nitrous acid, leading to potential thirdhand smoke hazards. *PNAS* **107**, 6576–6581, https://doi.org/10.1073/pnas.0912820107
14 Schick, S.F., Farraro, K.F., Perrino, C., Sleiman, M., van de Vossenberg, G., Trinh, M.P. et al. (2014) Thirdhand cigarette smoke in an experimental chamber: evidence of surface deposition of nicotine, nitrosamines and polycyclic aromatic hydrocarbons and de novo formation of NNK. *Tob. Control* **23**, 152–159, https://doi.org/10.1136/tobaccocontrol-2012-050915
15 Hang, B., Sarker, A.H., Havel, C., Saha, S., Hazra, T.K., Schick, S. et al. (2013) Thirdhand smoke causes DNA damage in human cells. *Mutagenesis* **28**, 381–391, https://doi.org/10.1093/mutage/get013
16 Dhall, S., Alamat, R., Castro, A., Sarker, A.H., Mao, J.H., Chan, A. et al. (2016) Tobacco toxins deposited on surfaces (third hand smoke) impair wound healing. *Clin. Sci.* **130**, 1269–1284, https://doi.org/10.1042/CS20160236
17 Martins-Green, M., Adhami, N., Frankos, M., Valdez, M., Goodwin, B., Lyubovitsky, J. et al. (2014) Cigarette smoke toxins deposited on surfaces: implications for human health. *PLoS One* **9**, e86391, https://doi.org/10.1371/journal.pone.0086391
18 Hang, B., Snijders, A.M., Huang, Y., Schick, S.F., Wang, P., Xia, Y. et al. (2017) Early exposure to thirdhand cigarette smoke affects body mass and the development of immunity in mice. *Sci. Rep.* **7**, 41915, https://doi.org/10.1038/srep41915
19 Xu, B., Chen, M., Yao, M., Ji, X., Mao, Z., Tang, W. et al. (2015) Metabolomics reveals metabolic changes in male reproductive cells exposed to thirdhand smoke. *Sci. Rep.* **5**, 15512, https://doi.org/10.1038/srep15512
20 Matt, G.E., Quintana, P.J., Zakarian, J.M., Fortmann, A.L., Chatfield, D.A., Hoh, E. et al. (2011) When smokers move out and non-smokers move in: residential thirdhand smoke pollution and exposure. *Tob. Control* **20**, e1, https://doi.org/10.1136/tc.2010.037382

Clinical Science (2018) **132** 475–488
https://doi.org/10.1042/CS20171521

21 Northrup, T.F., Khan, A.M., Jacob, P., Benowitz, 3rd, N.L., Hoh, E., Hovell, M.F. et al. (2016) Thirdhand smoke contamination in hospital settings: assessing exposure risk for vulnerable paediatric patients. *Tob. Control* **25**, 619–623, https://doi.org/10.1136/tobaccocontrol-2015-052506
22 Ramirez, N., Ozel, M.Z., Lewis, A.C., Marce, R.M., Borrull, F. and Hamilton, J.F. (2014) Exposure to nitrosamines in thirdhand tobacco smoke increases cancer risk in non-smokers. *Environ. Int.* **71**, 139–147, https://doi.org/10.1016/j.envint.2014.06.012
23 Whitehead, T.P., Havel, C., Metayer, C., Benowitz, N.L. and Jacob, 3rd, P. (2015) Tobacco alkaloids and tobacco-specific nitrosamines in dust from homes of smokeless tobacco users, active smokers, and nontobacco users. *Chem. Res. Toxicol.* **28**, 1007–1014, https://doi.org/10.1021/acs.chemrestox.5b00040
24 Bahl, V., Jacob, 3rd, P., Havel, C., Schick, S.F. and Talbot, P. (2014) Thirdhand cigarette smoke: factors affecting exposure and remediation. *PLoS One* **9**, e108258, https://doi.org/10.1371/journal.pone.0108258
25 Dobin, A., Davis, C.A., Schlesinger, F., Drenkow, J., Zaleski, C., Jha, S. et al. (2013) STAR: ultrafast universal RNA-seq aligner. *Bioinformatics* **29**, 15–21, https://doi.org/10.1093/bioinformatics/bts635
26 Anders, S., Pyl, P.T. and Huber, W. (2014) HTseq – A Python framework to work with high-throughput sequencing data. *bioRxiv*
27 Loureiro, J., Rodriguez, E., Doležel, J. and Santos, C. (2006) Comparison of four nuclear isolation buffers for plant DNA flow cytometry. *Ann. Bot. (Lond.)* **98**, 679–689, https://doi.org/10.1093/aob/mcl141
28 Love, M.I., Huber, W. and Anders, S. (2014) Moderated estimation of fold change and dispersion for RNA-seq data with DESeq2. *Genome Biol.* **15**, 550, https://doi.org/10.1186/s13059-014-0550-8
29 Wang, Y., Wen, M., Kwon, Y., Xu, Y., Liu, Y., Zhang, P. et al. (2014) CUL4A induces epithelial-mesenchymal transition and promotes cancer metastasis by regulating ZEB1 expression. *Cancer Res.* **74**, 520–531, https://doi.org/10.1158/0008-5472.CAN-13-2182
30 Bosse, Y., Postma, D.S., Sin, D.D., Lamontagne, M., Couture, C., Gaudreault, N. et al. (2012) Molecular signature of smoking in human lung tissues. *Cancer Res.* **72**, 3753–3763, https://doi.org/10.1158/0008-5472.CAN-12-1160
31 Rogakou, E.P., Pilch, D.R., Orr, A.H., Ivanova, V.S. and Bonner, W.M. (1998) DNA double-stranded breaks induce histone H2AX phosphorylation on serine 139. *J. Biol. Chem.* **273**, 5858–5868, https://doi.org/10.1074/jbc.273.10.5858
32 Hecht, S.S. (1999) Tobacco smoke carcinogens and lung cancer. *J. Natl. Cancer Inst.* **91**, 1194–1210, https://doi.org/10.1093/jnci/91.14.1194
33 Shimkin, M.B. and Stoner, G.D. (1975) Lung tumors in mice: application to carcinogenesis bioassay. *Adv. Cancer Res.* **21**, 1–58, https://doi.org/10.1016/S0065-230X(08)60970-7
34 Hecht, S.S., Isaacs, S. and Trushin, N. (1994) Lung tumor induction in A/J mice by the tobacco smoke carcinogens 4-(methylnitrosamino)-1-(3-pyridyl)-1-butanone and benzo[a]pyrene: a potentially useful model for evaluation of chemopreventive agents. *Carcinogenesis* **15**, 2721–2725, https://doi.org/10.1093/carcin/15.12.2721
35 Bogen, K.T. and Witschi, H. (2002) Lung tumors in A/J mice exposed to environmental tobacco smoke: estimated potency and implied human risk. *Carcinogenesis* **23**, 511–519, https://doi.org/10.1093/carcin/23.3.511
36 Peterson, L.A., Thomson, N.M., Crankshaw, D.L., Donaldson, E.E. and Kenney, P.J. (2001) Interactions between methylating and pyridyloxobutylating agents in A/J mouse lungs: implications for 4-(methylnitrosamino)-1-(3-pyridyl)-1-butanone-induced lung tumorigenesis. *Cancer Res.* **61**, 5757–5763
37 Hang, B. (2010) Formation and repair of tobacco carcinogen-derived bulky DNA adducts. *J. Nucleic Acids* **2010**, 709521, https://doi.org/10.4061/2010/709521
38 Hang, B., Iavarone, A., Havel, C., Jacob, P., Villalta, P., Matter, B. et al. (2014) NNA, a thirdhand smoke constituent, induces DNA damage in vitro and in human cells. In *Proceedings of the 247th National Meeting of the American-Chemical-Society*. **247**
39 Pfeifer, G.P., Denissenko, M.F., Olivier, M., Tretyakova, N., Hecht, S.S. and Hainaut, P. (2002) Tobacco smoke carcinogens, DNA damage and p53 mutations in smoking-associated cancers. *Oncogene* **21**, 7435–7451, https://doi.org/10.1038/sj.onc.1205803
40 Jackson, S.P. (2002) Sensing and repairing DNA double-strand breaks. *Carcinogenesis* **23**, 687–696, https://doi.org/10.1093/carcin/23.5.687
41 Khanna, K.K. and Jackson, S.P. (2001) DNA double-strand breaks: signaling, repair and the cancer connection. *Nat. Genet.* **27**, 247–254, https://doi.org/10.1038/85798

Figure S1

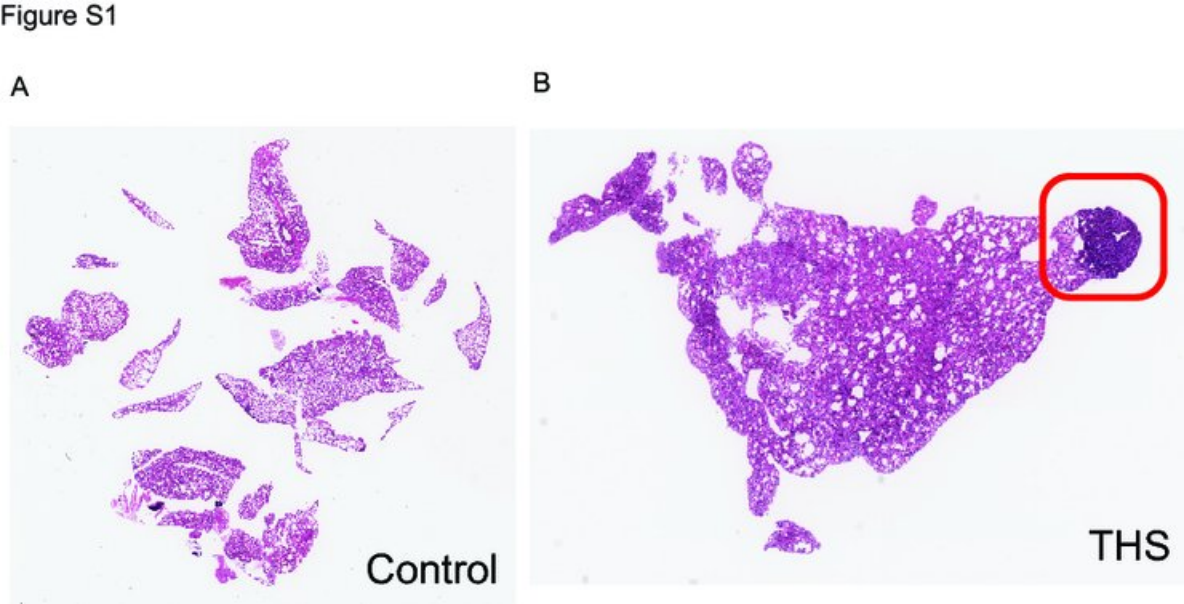

Figure S2

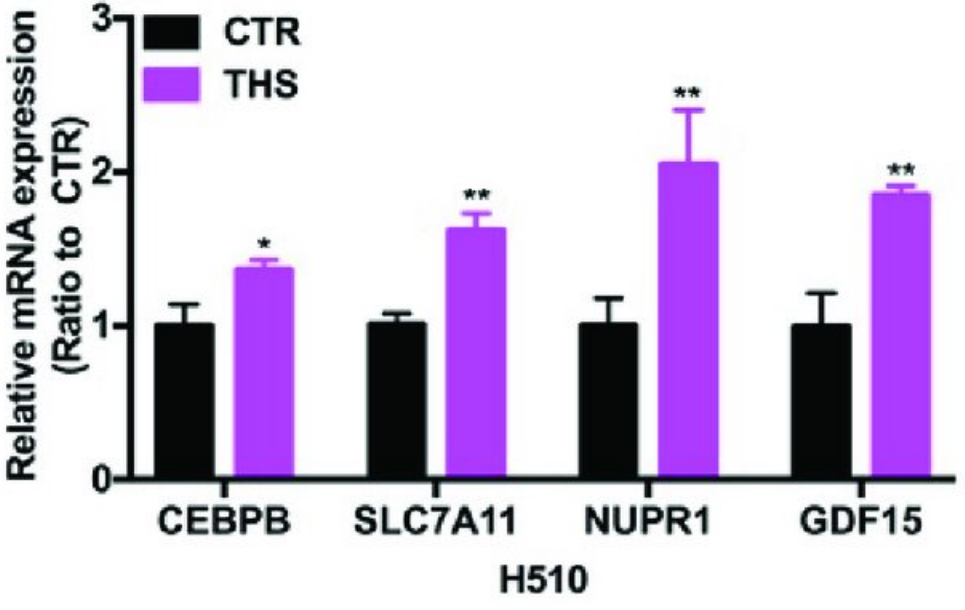
Relative mRNA expression
(Ratio to CTR)
3
2
1
0
CTR
THS
*
**
**
**
CEBPB
SLC7A11
NUPR1
GDF15
H510

Figure S3

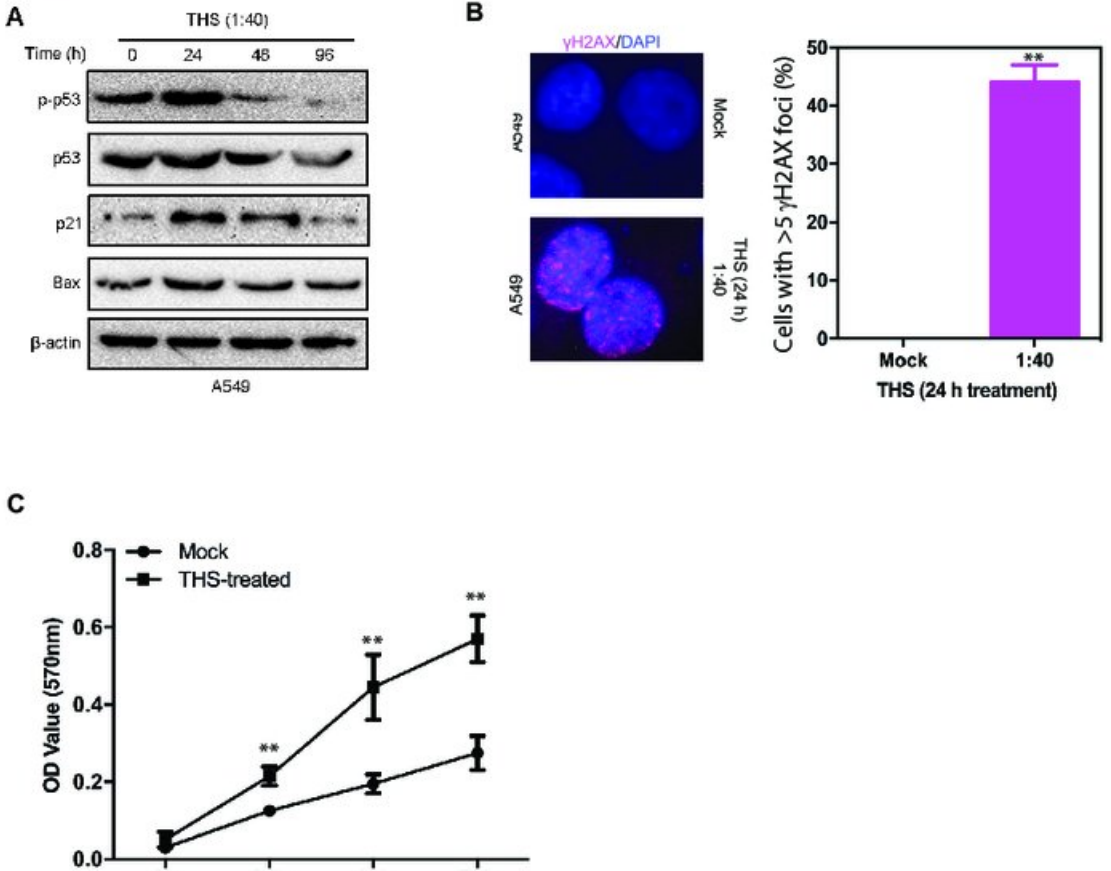
A
THS (1:40)
Time (h)
0
24
48
96
p-p53
p53
p21
Bax
β-actin
A549
B
γH2AX/DAPI
Mock
THS (24 h) 1:40
A549
Cells with >5 γH2AX foci (%)
50
40
30
20
10
0
**
Mock
1:40
THS (24 h treatment)
C
Mock
THS-treated
OD Value (570nm)
0.8
0.6
0.4
0.2
0.0
**
**
**
0h
24h
48h
72h
A549

Figure S4

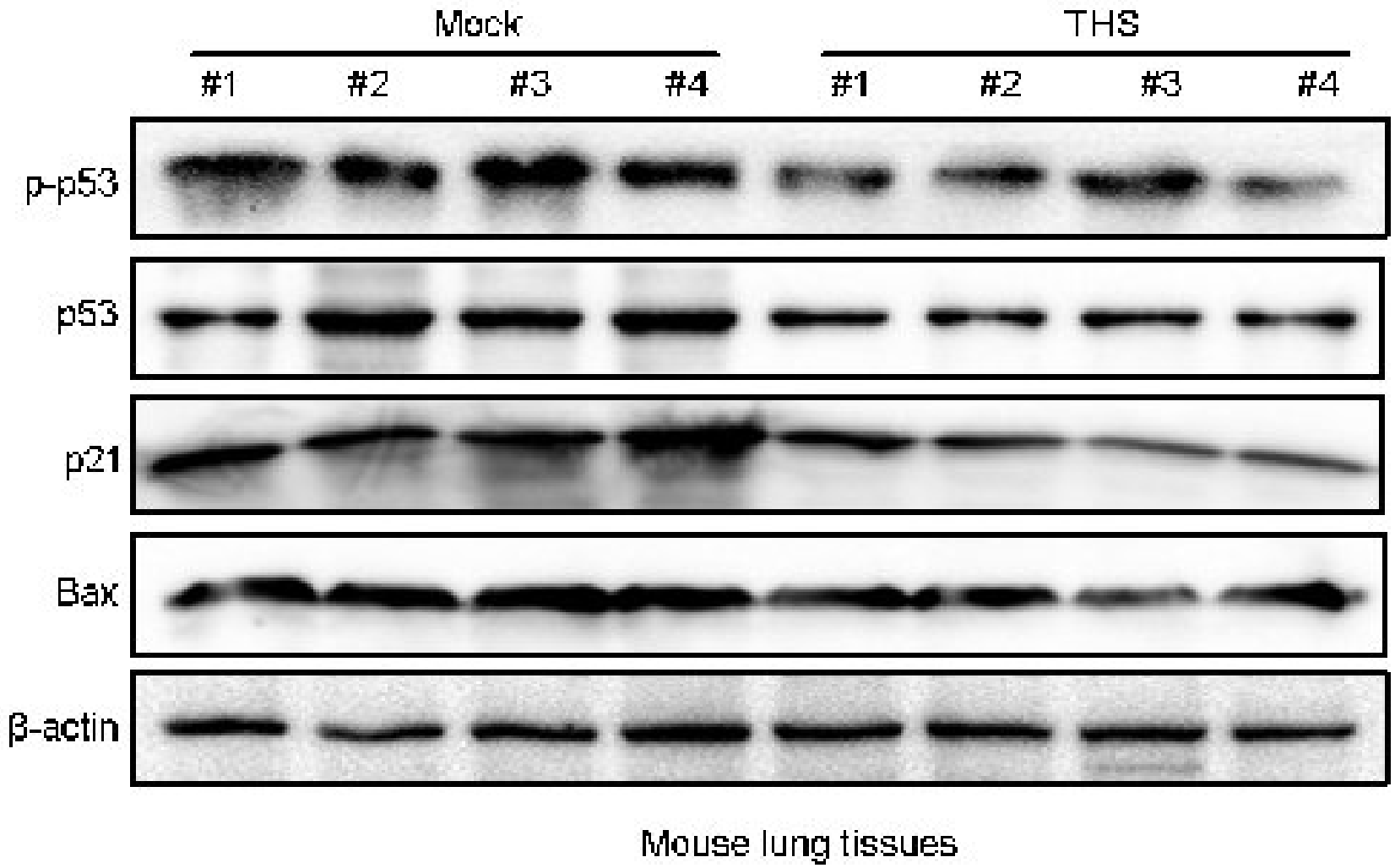
Mock
THS
#1
#2
#3
#4
#1
#2
#3
#4
p-p53
p53
p21
Bax
β-actin
Mouse lung tissues

FIgure S5

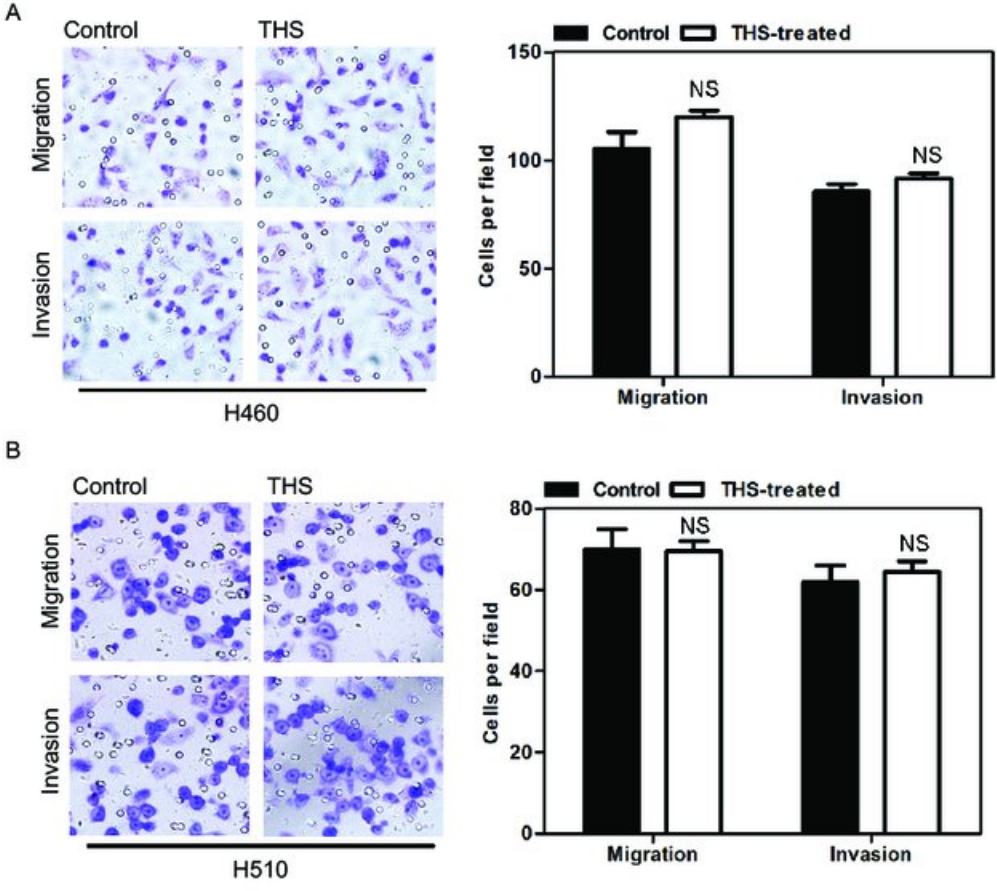
A
Control
THS
Migration
Invasion
H460
Control
THS-treated
150
100
50
0
Cells per field
NS
NS
Migration
Invasion
B
Control
THS
Migration
Invasion
H510
Control
THS-treated
80
60
40
20
0
Cells per field
NS
NS
Migration
Invasion